

1 Draft genomes of the three northern hemisphere
2 blue mussel lineages: North and South European
3 *Mytilus edulis* and Mediterranean *Mytilus*
4 *galloprovincialis*.

5 Alexis Simon^{1,*}, Christine Arbiol¹, and Nicolas Bierne¹

6 ¹CNRS, Univ Montpellier, ...

7 June 23, 2022

8 **Abstract**

9 Using the 10X chromium long reads technology, we provide draft genomes
10 for three closely related blue mussel species from the *Mytilus* species complex.
11 The objective was to produce affordable genomic resources for population and
12 evolutionary genomic studies. Genomes are fragmented but represent a large
13 portion of the genome, with good sizes and BUSCO scores.

14 **Keywords:** *Mytilus edulis*, *Mytilus galloprovincialis*, Genome assembly, 10X chromium

15 * **Corresponding author:** alexis.simon@normalesup.org

1 Rationale and objectives

The *Mytilus* species complex has been a model system in population genetics, adaptation, hybridization and speciation since genetic variants could be identified (Ahmad et al., 1977; Bierne et al., 2003; Fraïsse et al., 2016; Koehn & Mitton, 1972; Milkman & Beaty, 1970; Quesada, Wenne, et al., 1995; Simon et al., 2021; Skibinski et al., 1978).

The *Mytilus* species complex is composed of three taxonomically recognized and partially reproductively isolated species in the northern hemisphere, *Mytilus edulis*, *M. galloprovincialis* and *M. trossulus*. Within each species, evolutionary relevant lineages can be identified. Two lineages of *M. galloprovincialis* can be identified, one Atlantic lineage and one Mediterranean lineage separated by a hybrid zone along the Almeria-Oran front (El Ayari et al., 2019; Fraïsse et al., 2016; Quesada, Zapata, et al., 1995). Three lineages of *M. edulis* can be identified: (i) an American lineage, (ii) a Southern European lineage, and (iii) a Northern European lineage (Fraïsse et al., 2016; Simon et al., 2020).

As an effort to diversify the genomic resources available for the *Mytilus* species complex, we assembled and annotate the genomes of three lineages using the 10X chromium technology. While our assemblies were initially fragmented due to the high level of heterozygosity, we leveraged the existence of a chromosome scale assembly of a sister species to scaffold our assemblies against it. We obtained assemblies equivalent to published ones in term of completeness for three new lineages of the species complex using a low sequencing budget and publicly available data. The resources produced and the assembly pipeline are freely available for use by the community.

2 Methods

General notes: The entire assembly was carried out using a Snakemake (Mölder et al., 2021) pipeline available on github at https://github.com/alxsimon/assembly_10x. Where deemed important, parameters are given in the text. For brevity and simplicity, not all information might be available in the text. However, all parameters, software versions and steps are retrievable from the repository.

Important caveat: The assembled genome of MeduEUN (*M. edulis* Northern lineage) was initially thought to be *M. trossulus*. Therefore some assembly and annotation steps wrongly used *M. trossulus* transcriptomes. While this is not ideal, we think results have not been strongly impacted by this issue.

2.1 Biological material and DNA extraction

One individual for each species of interest was collected and processed fresh.

Collection locations:

- *M. galloprovincialis* Mediterranean MgalMED; Sète, France

- *M. edulis* Southern European MeduEUS; ???
- *M. edulis* Northern Europe MeduEUN; ???

Whole mussels were placed in 50 mL falcon tubes containing 25 mL of TNES-Urea solution and incubated for 4-6 weeks at room temperature (TNES-Urea: 10 mM Tris-HCl pH 7.4; 120 mM NaCl; 10 mM EDTA pH 8.0; 0.5% SDS; 4 M urea).

After this period of pre-treatment at ambient temperature, proteinase K was added at a final concentration of 150 µg/mL and the solution was incubated overnight at 56°C.

High Molecular weight genomic DNA was extracted following Nakayama et al. (1994). We used a 15 mL Phase Lock Gel Heavy extraction with 3 steps of phenol/chloroform/isoamylalcohol (25/24/1) Tris pH 8.1 followed by 2 chloroform extractions. After the last extraction, the aqueous supernatant was precipitated with 2 volumes of 100% EtOH and the pellet was hooked from the solution with a sterile glass Pasteur pipette. The pellet was rinsed several times in 80% EtOH before being dried at room temperature.

DNA was resuspended with an appropriate volume of biomolecular water at 65°C for several hours, the duration of this incubation depending on the size of the granules. DNA was then stored at 4°C.

Prior to the construction of the DNA libraries, DNA was repaired with NEBNext FFPE DNA Repair Mix according to the manufacturer's instructions.

2.2 Library preparation and sequencing

The 10X chromium library preparation and sequencing was subcontracted to the MGX platform (Montpellier, France). The 10X linked reads libraries for each individual were produced following the 10X Genomics Genome Reagent Kit (*Genome Solution*) protocol using a Chromium microfluidic chip. Libraries were subsequently sequenced on an Illumina NovaSeq 6000 with an S4 flowcell.

2.3 Preprocessing 10X reads

We preprocessed 10X reads using the following pipeline for use in several algorithms (section 2.4). We first removed duplicate reads using `Nubeam-dedup` (Dai and Guan, 2020; commit 25dd385). We then used `proc10xG` (<https://github.com/ucdavis-bioinformatics/proc10xG>; commit 7afbfcf) to split the reads from their 10X barcodes for further processing. We used a custom filtering step designed to remove under- and over-represented barcodes and their associated reads from the data (figs. S1 to S3, `filter_barcodes.R` script, see **Bary\&Gagnaire??**). [[Add supfigs of filter_barcodes]]. Reads were additionally filtered with `fastp` (v0.20.1; Chen et al., 2018) with the main objective to remove poly-G tails created by the Illumina Novaseq sequencing technology. We obtained at this point reads equivalent to a short-read sequencing run, usable in some parts of the assembly and quality control pipeline. Additionally, to obtain reads compatible to 10X genomics tools, we filtered and reassembled reads with their 10X barcodes in `proc10xG` using the `filter_10xReads.py` and `regen_10xReads.py` scripts.

2.4 Initial genome assemblies

For each genome we used Supernova v2.1.1 (Weisenfeld et al., 2017) to assemble raw 10X reads. To avoid hard stops in Supernova due to both data quantity slightly under 10X genomics recommendations and an overestimation of genome size by Supernova, we used all available reads (`--maxreads='all'`) and accepted extreme coverage (`--accept-extreme-coverage`). We produced every style of Fasta output available in Supernova but only used the pseudo-haploid output in the following pipeline.

To remove duplicate haplotypes in the assemblies, we followed the `purge_dups` pipeline (Guan et al., 2020; commit e1934bb). We first used the `longranger` v2.2.2 align algorithm to map preprocessed reads (section 2.3) to the pseudo-haploid genomes to use in the `ngscstat` step. `Minimap2` (v2.17; Li, 2017) was used in the contig self-mapping step. We obtained the purged assemblies using the `get_seqs` steps without restricting the purging to the end of contigs (without the `-e` option).

We used AGOUTI (<https://github.com/svm-zhang/AGOUTI>; commit a7e65d6; Zhang et al., 2016) to improve scaffolding by using paired end RNA-seq reads. For each species, a different set of published transcriptomes were used (Supplementary Table [...] for accessions). AGOUTI require a gene prediction as input in addition to RNA-seq reads. We used Augustus (v3.3.3; Stanke et al., 2008) to produce an intermediate annotation for each assembly using the *Caenorhabditis* model. RNA-seq reads were first cleaned using `rcorrector` (v1.0.4; Song and Florea, 2015) and `trimalore` (v0.6.6; https://www.bioinformatics.babraham.ac.uk/projects/trim_galore; `--quality 20 --stringency 1 -e 0.1 --length 70`). RNA-seq reads were mapped independently using `bwa-mem2` (v2.2.1; Vasimuddin Md et al., 2019), and then merged as a common bam file for each assembly with `samtools` (v1.12; Li et al., 2009). Finally, the AGOUTI scaffolding pipeline was run using the gene prediction and mapped RNA-seq reads (`-minMQ 20 -maxFracMM 0.05`; using `python` v2.7.15 and `samtools` v1.10 for compatibility).

As a last step, we ran *Blobtoolkit* (v2.4.0; Challis et al., 2020) on the three assemblies to evaluate quality and potential contamination levels. We used a custom script (`btk_conta_extraction.py`) to filter the assembly contigs based on the taxids found by the *Blobtoolkit* pipeline to remove the most obvious contaminations. Contigs matching taxids associated with viruses, bacteria and non-mollusca eukaryotes were removed. More specifically contigs for were removed for virus contamination if they presented a hit percentage of more than 10 % of their length. Contigs were removed for eukaryote contamination only when presenting only hits to taxa outside Mollusca on more than 10 % of their length. The list of retained contigs was used to filter the fasta assembly file using `seqkit` (v0.13.2; Shen et al., 2016).

2.5 Scaffolding on the *Mytilus coruscus* genome

At the time of assembly, the closest relative of the *Mytilus* species of interest with a chromosome scale assembly was *Mytilus coruscus* (GCA_017311375.1; Yang et al., 2021). Given the conserved number of 14 chromosomes in the *Mytilus* genus, we decided to scaffold our contigs on this high quality reference. Additionally, we had Oxford Nanopore reads for the MeduEUN individual. We used `minimap2` (v2.17; Li, 2017) and `LRScaf` (v1.1.10; <https://github.com/shingocat/lrscaf>) to first improve the MeduEUN assembly with this small amount of long reads.

Then for each assembly, we ran the scaffolder RagTag (v1.1.1; Alonge et al., 2021) to position contigs on the *M. coruscus* chromosomal assembly.

A final polishing step was performed using Pilon (v1.24; Walker et al., 2014). Pilon attempts to improve the assembly based on mapped read information (gap filling and error corrections). We used bwa-mem2 to map the debarcoded and filtered 10X reads (section 2.3). In addition, Oxford Nanopore reads for MeduEUN were also used in Pilon for the given assembly.

2.6 Repeats

We masked repeats for the purpose of annotation using RepeatModeler (v2.0.1; Flynn et al., 2020) and RepeatMasker (v4.1.2-p1; Smit et al., 2013–2015) through the TETools DFAM container (v1.3.1; <https://hub.docker.com/r/dfam/tetools>). We first built repeat databases for each of five assemblies MgalMED, MeduEUS, MeduEUN, *M. coruscus* (GCA_017311375.1; Yang et al., 2021) and *M. galloprovincialis* from the Atlantic (GCA_g00618805.1; Gerdol et al., 2020). Then, we built a common *Mytilus* database of repeats by merging those five databases using cd-hit (v4.8.1; Fu et al., 2012). We used the same options as used by default in RepeatModeler: -aS 0.8 -c 0.8 -g 1 -G 0 -A 80 -M 10000. Finally, soft repeat masking was performed on the assemblies with RepeatMasker using the merged database.

2.7 Annotation

To obtain an annotation for each assembly, we used both database and RNA-seq information. We used Braker2 (v2.1.6; Brůna et al., 2021) as an initial step, using both a protein database and RNA-seq reads (preprocessed in section 2.4). To build the protein database, we used all *Mollusca* proteins (taxid 6447) from OrthoDB (v10.1; Kriventseva et al., 2019). To provide gene presence hints, we mapped all RNA-seq reads for each species using HISAT2 (v2.2.1; Kim et al., 2019).

We used the Mantis pipeline (<https://github.com/PedroMTQ/mantis>; commit c6cb597; Queirós et al., 2021) to obtain consensus annotations of genes based on multiple databases. Protein sequences for each assembly were built from the Braker2 annotation using the python module gff3tool (v2).

2.8 NCBI submission

The NCBI submission process identified a few errors that needed correcting. A small number of adaptor sequences and duplicates were removed to comply with NCBI requirements (see the rule ncbi_submission_changes.smk in the pipeline for more details). Assemblies are available under the following accessions: JAKGDF000000000 for MgalMED, JAKGDG000000000 for MeduEUS, and JAKGDH000000000 for MeduEUN.

2.9 Quality assessments and comparisons

Preprocessed 10X reads (section 2.3) were used to first estimate genome size and heterozygosities of the three individuals. We used the reference free k-mer based method `GenomeScope` (<https://github.com/tbenavi1/genomescope2.0>; commit 5034ed4; Ranallo-Benavidez et al., 2020) and the fork of the `KMC` k-mer counting program (<https://github.com/tbenavi1/KMC>; commit 1df71f6).

Assembly statistics were computed with the python module `assembly_stats` (v0.1.4; Trizna, 2020).

To assess the remaining level of duplication in the assemblies, we used the program `KAT` (v2.4.2; Mapleson et al., 2017) to compare k-mer spectra from reads (preprocessed 10X) and from the assembly.

Finally, gene completion analyses were carried out using `BUSCO` (v5.1.1; Manni et al., 2021). We used both a Metazoan (`metazoa_odb10.2021-02-24`) and Molluscan (`mollusca_odb10.2020-08-08`) database to assess and compare new and published assemblies. We compared our assemblies to the following published ones:

- *M. coruscus*, GCA_017311375.1, Yang et al. (2021);
- *M. galloprovincialis* from the Atlantic lineage, GCA_900618805.1, Gerdol et al. (2020);
- *M. edulis* from the Southern European lineage, GCA_905397895.1, Corrochano-Fraile et al. (2021)
- *M. edulis* from the American lineage, GCA_019925275.1.

2.10 Phylogenetic species tree

We compiled protein sequences from published *Mytilus* genomes and transcriptomes, in addition to the current three genomes and annotations, to build a species tree. We used transcriptomes produced in Popovic and Riginos (2020) for American *M. edulis*, Mediterranean *M. galloprovincialis*, *M. trossulus*, *M. californianus*. Transcriptomes were translated using the `seqkit` program (v2.2.0; Shen et al., 2016). We used genomes and associated annotations of *M. coruscus* (GCA_017311375.1; Yang et al. (2021)), Southern European *M. edulis* (GCA_905397895.1; Corrochano-Fraile et al. (2021)), Atlantic *M. galloprovincialis* (GCA_900618805.1; Gerdol et al. (2020)), and American *M. edulis* (GCA_019925275.1; annotation as personal communication of Tiago Hori, PEIMSO). For GCA_019925275.1, protein sequences were retrieved from the fasta and gff files using the python module `gff3tool` (v2.1.0).

We used `Orthofinder` (v2.5.2; Emms and Kelly, 2015, 2019) to find orthogroups and orthologue genes. Species tree was inferred using the MSA method of `Orthofinder` (Emms & Kelly, 2018) and `IQ-TREE` (v2.2.0_beta; Minh et al., 2020) tree inference.

3 Results and discussion

We introduce here newly assembled genomes from three lineages of the *Mytilus* species complex. With a limited budget of $\sim 3000\text{€}$ per genome, we managed to produce draft genomes of enough quality to be useful in applications such as population genomics and genetics. The method of 10X chromium pseudo-long reads combined with scaffolding using published data provided a quality comparable to published assemblies for *Mytilus* species.

The pre-assembly k-mer analysis carried out using GenomeScope (using 21-mers) showed that, as expected, the genomes were highly heterozygous with values going from 3.49 to 8.77 % (fig. 1). GenomeScope provide a bad fit and estimation in the case of the MeduEUS data due to a reduced coverage of the genome in that case, compared to the two other assemblies.

Highly heterozygous genomes brings the risk of having a large number of duplicate contigs due to the separate assembly of the two alleles from a same locus. For this reason, we used the `purge_dups` pipeline to try removing a maximum of such bias. This procedure reduced the number of complete duplicated genes in all assemblies (fig. S4, v1 to v4).

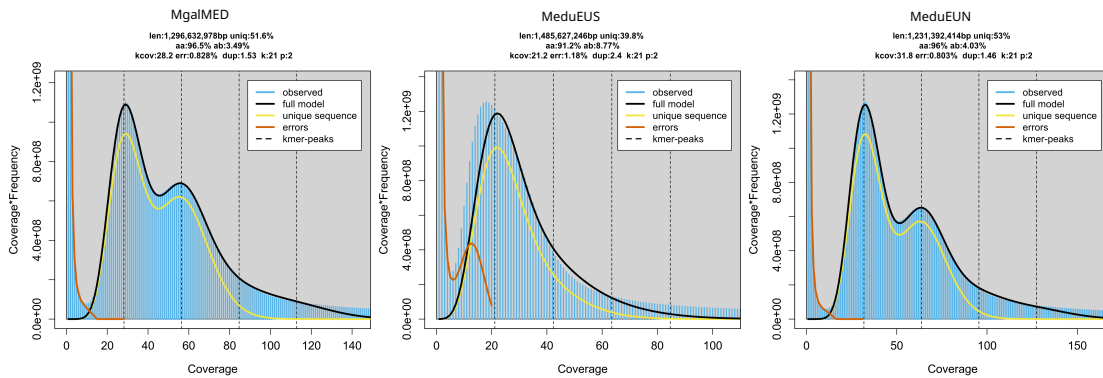


Figure 1: k-mer profile plots computed with 21-mers using GenomeScope. Coverage histogram of the k-mers in blue. Lines represent the fit of the GenomeScope models. len: inferred genome length; uniq: percentage of the genome that is unique, aa: overall homozygosity; ab: overall heterozygosity; kcov: mean k-mer coverage for heterozygous bases; err: reads error rate; dup: average rate of read duplication; k: k-mer size; p: ploidy.

Table 1: Assembly statistics comparisons. C for contigs and S for scaffolds.

assembly	C.L50	C.N50	C.median	C.sequence_count	S.L50	S.N50	S.gc_content	S.median	S.sequence_count	S.total_bps
Mcor_GCA017311375	261	1481111	42077	6449	6	99542347	32.4	21293	4434	1566529938
MgalATL_GCA900618805	4922	77035	39489	22922	1903	207642	32.1	77568	10577	1282208009
MeduEUS_GCA905397895	977	511485	184638	5966	464	1097279	32.2	292104	3339	1827085763
MeduAM_GCA019925415	835	490737	62522	9686	6	116503180	32.3	28931	1119	1651313236
MgalMED_v7	16906	26323	7475	115913	9	71952646	32.1	4531	41122	1658656017
MeduEUS_v7	24467	23624	6478	169324	415	228263	34.6	4999	73616	2076685641
MeduEUN_v7	15862	29157	8961	105892	9	77102752	32.1	6164	28220	1764246486

To assess the completeness of our assemblies, we compared them to four *Mytilus* published assemblies on the basis of a Metazoan and a Molluscan set of single copy orthologous genes using BUSCO (fig. 2). Overall, we show that our assemblies are equivalent to the published ones in terms of completeness.

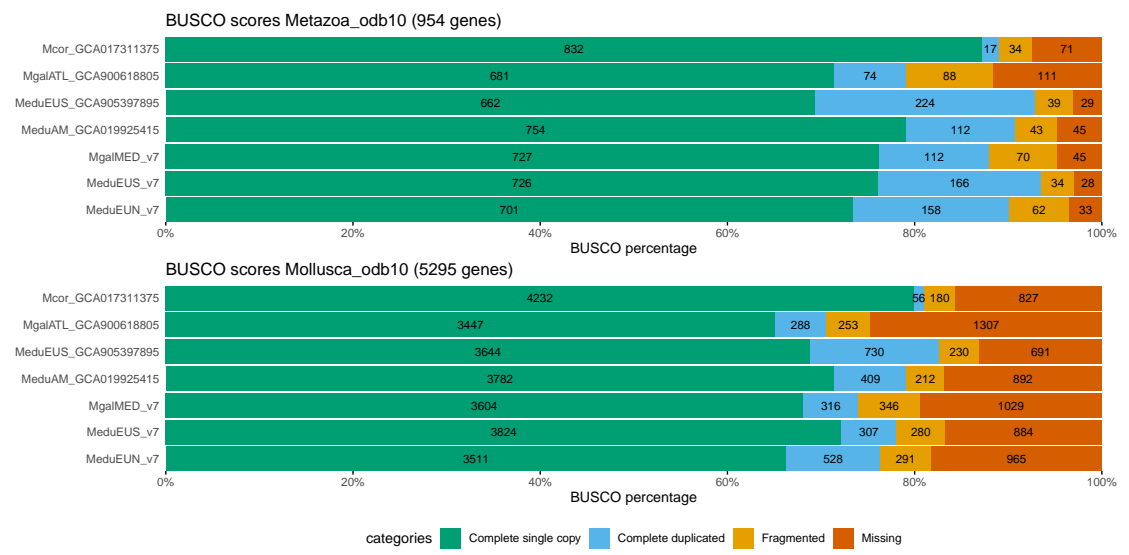


Figure 2: Busco scores

The species tree (fig. 3) shows that the assemblies and the published genomes and transcriptomes are clustering as expected. Orthofinder provides

provide the orthogroups somewhere

a resource of single-copy orthogroups across a large part the *Mytilus* species complex.

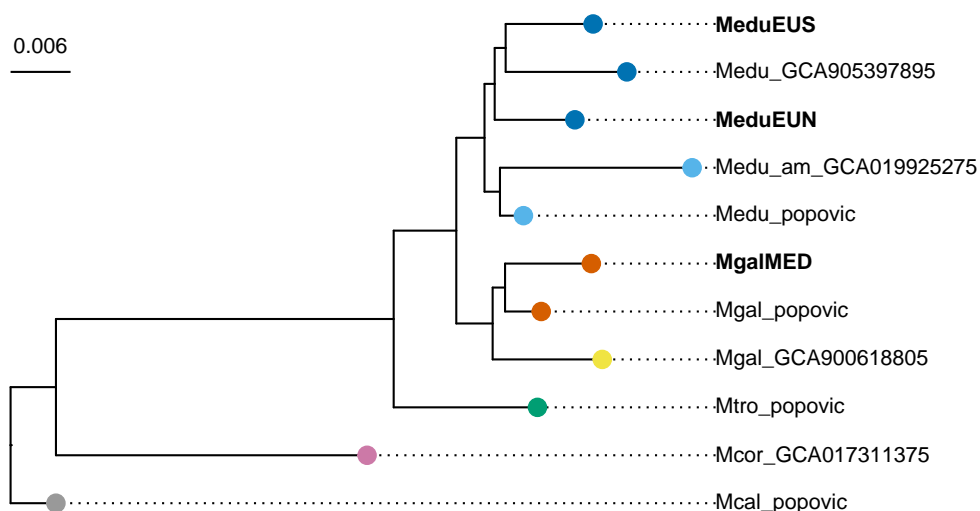


Figure 3: Species tree using 1300 orthogroups with minimum of 81.8% of species having single-copy genes in any orthogroup. Color coding – dark blue: *M. edulis* Europe, light blue: *M. edulis* America, red: *M. galloprovincialis* Mediterranean Sea, yellow: *M. galloprovincialis* Atlantic, green: *M. trossulus*, pink: *M. coruscus*, gray: *M. californianus*.

Acknowledgements

We thank [XXX]. AS was supported by the ANR grant [XXX] and by the National Institute of General Medical Sciences of the National Institutes of Health (grants NIH R01 GM108779 and R35 GM136290 to Dr Graham Coop).

References

- Ahmad, M., Skibinski, D. O. F., & Beardmore, J. A. (1977). An estimate of the amount of genetic variation in the common mussel *Mytilus edulis*. *Biochemical Genetics*, 15(9-10), 833–846. <https://doi.org/10.1007/BF00483980>
- Alonge, M., Lebeigle, L., Kirsche, M., Aganezov, S., Wang, X., Lippman, Z. B., Schatz, M. C., & Soyk, S. (2021). Automated assembly scaffolding elevates a new tomato system for high-throughput genome editing. *bioRxiv*, 2021.11.18.469135. <https://doi.org/10.1101/2021.11.18.469135>
- Bierne, N., Borsa, P., Daguin, C., Jollivet, D., Viard, F., Bonhomme, F., & David, P. (2003). Introgression patterns in the mosaic hybrid zone between *Mytilus edulis* and *M. galloprovincialis*. *Molecular Ecology*, 12(2), 447–461. <https://doi.org/10.1046/j.1365-294X.2003.01730.x>
- Brůna, T., Hoff, K. J., Lomsadze, A., Stanke, M., & Borodovsky, M. (2021). BRAKER2: Automatic eukaryotic genome annotation with GeneMark-EP+ and AUGUSTUS supported by a protein database. *NAR Genomics and Bioinformatics*, 3(1), lqaa108. <https://doi.org/10.1093/nargab/lqaa108>
- Challis, R., Richards, E., Rajan, J., Cochrane, G., & Blaxter, M. (2020). BlobToolKit – Interactive Quality Assessment of Genome Assemblies. *G3 Genes|Genomes|Genetics*, 10(4), 1361–1374. <https://doi.org/10.1534/g3.119.400908>

- Chen, S., Zhou, Y., Chen, Y., & Gu, J. (2018). Fastp: An ultra-fast all-in-one FASTQ preprocessor. *Bioinformatics*, 34, i884–i890. <https://doi.org/10.1093/bioinformatics/bty560>
- Corrochano-Fraile, A., Davie, A., & Carboni, S. (2021). Evidence of multiple genome duplication events in *Mytilus* evolution. *bioRxiv*. <https://doi.org/10.1101/2021.08.17.456601>
- Dai, H., & Guan, Y. (2020). Nubeam-dedup: A fast and RAM-efficient tool to de-duplicate sequencing reads without mapping (I. Birol, Ed.). *Bioinformatics*, 36(10), 3254–3256. <https://doi.org/10.1093/bioinformatics/btaa112>
- El Ayari, T., Trigui El Menif, N., Hamer, B., Cahill, A. E., & Bierne, N. (2019). The hidden side of a major marine biogeographic boundary: A wide mosaic hybrid zone at the Atlantic–Mediterranean divide reveals the complex interaction between natural and genetic barriers in mussels. *Heredity*, 122, 770–784. <https://doi.org/10.1038/s41437-018-0174-y>
- Emms, D. M., & Kelly, S. (2018). STAG: Species Tree Inference from All Genes. *bioRxiv*, 267914. <https://doi.org/10.1101/267914>
- Emms, D. M., & Kelly, S. (2015). OrthoFinder: Solving fundamental biases in whole genome comparisons dramatically improves orthogroup inference accuracy. *Genome Biology*, 16(1), 157. <https://doi.org/10.1186/s13059-015-0721-2>
- Emms, D. M., & Kelly, S. (2019). OrthoFinder: Phylogenetic orthology inference for comparative genomics. *Genome Biology*, 20(1), 238. <https://doi.org/10.1186/s13059-019-1832-y>
- Flynn, J. M., Hubley, R., Goubert, C., Rosen, J., Clark, A. G., Feschotte, C., & Smit, A. F. (2020). RepeatModeler2 for automated genomic discovery of transposable element families. *Proceedings of the National Academy of Sciences*, 117(17), 9451–9457. <https://doi.org/10.1073/pnas.1921046117>
- Fraïsse, C., Belkhir, K., Welch, J. J., & Bierne, N. (2016). Local interspecies introgression is the main cause of extreme levels of intraspecific differentiation in mussels. *Molecular Ecology*, 25(1), 269–286. <https://doi.org/10.1111/mec.13299>
- Fu, L., Niu, B., Zhu, Z., Wu, S., & Li, W. (2012). CD-HIT: Accelerated for clustering the next-generation sequencing data. *Bioinformatics*, 28(23), 3150–3152. <https://doi.org/10.1093/bioinformatics/bts565>
- Gerdol, M., Moreira, R., Cruz, F., Gómez-Garrido, J., Vlasova, A., Rosani, U., Venier, P., Naranjo-Ortiz, M. A., Murgarella, M., Greco, S., Balseiro, P., Corvelo, A., Frias, L., Gut, M., Gabaldón, T., Pallavicini, A., Canchaya, C., Novoa, B., Alioto, T. S., ... Figueras, A. (2020). Massive gene presence-absence variation shapes an open pan-genome in the Mediterranean mussel. *Genome Biology*, 21(1), 275. <https://doi.org/10.1186/s13059-020-02180-3>
- Guan, D., McCarthy, S. A., Wood, J., Howe, K., Wang, Y., & Durbin, R. (2020). Identifying and removing haplotypic duplication in primary genome assemblies. *Bioinformatics*, 36(9), 2896–2898. <https://doi.org/10.1093/bioinformatics/btaa025>
- Kim, D., Paggi, J. M., Park, C., Bennett, C., & Salzberg, S. L. (2019). Graph-based genome alignment and genotyping with HISAT2 and HISAT-genotype. *Nature Biotechnology*, 37(8), 907–915. <https://doi.org/10.1038/s41587-019-0201-4>
- Koehn, R. K., & Mitton, J. B. (1972). Population Genetics of Marine Pelecypods. I. Ecological Heterogeneity and Evolutionary Strategy at an Enzyme Locus. *The American Naturalist*, 106(947), 47–56. <https://doi.org/10.1086/282750>
- Kriventseva, E. V., Kuznetsov, D., Tegenfeldt, F., Manni, M., Dias, R., Simão, F. A., & Zdobnov, E. M. (2019). OrthoDB v10: Sampling the diversity of animal, plant, fungal,

- protist, bacterial and viral genomes for evolutionary and functional annotations of orthologs. *Nucleic Acids Research*, 47(D1), D807–D811. <https://doi.org/10.1093/nar/gky1053>
- Li, H., Handsaker, B., Wysoker, A., Fennell, T., Ruan, J., Homer, N., Marth, G., Abecasis, G., Durbin, R., & 1000 Genome Project Data Processing Subgroup. (2009). The Sequence Alignment/Map format and SAMtools. *Bioinformatics*, 25(16), 2078–2079. <https://doi.org/10.1093/bioinformatics/btp352>
- Li, H. (2017). *Minimap2: Pairwise alignment for nucleotide sequences*.
- Manni, M., Berkeley, M. R., Seppey, M., Simão, F. A., & Zdobnov, E. M. (2021). BUSCO Update: Novel and Streamlined Workflows along with Broader and Deeper Phylogenetic Coverage for Scoring of Eukaryotic, Prokaryotic, and Viral Genomes. *Molecular Biology and Evolution*, 38(10), 4647–4654. <https://doi.org/10.1093/molbev/msab199>
- Mapleson, D., Garcia Accinelli, G., Kettleborough, G., Wright, J., & Clavijo, B. J. (2017). KAT: A K-mer analysis toolkit to quality control NGS datasets and genome assemblies. *Bioinformatics*, 33(4), 574–576. <https://doi.org/10.1093/bioinformatics/btw663>
- Milkman, R., & Beaty, L. (1970). Large-Scale Electrophoretic Studies of Allelic Variation in *Mytilus edulis*. *Biological Bulletin*, 139, 430.
- Minh, B. Q., Schmidt, H. A., Chernomor, O., Schrempf, D., Woodhams, M. D., von Haeseler, A., & Lanfear, R. (2020). IQ-TREE 2: New Models and Efficient Methods for Phylogenetic Inference in the Genomic Era. *Molecular Biology and Evolution*, 37(5), 1530–1534. <https://doi.org/10.1093/molbev/msaa015>
- Mölder, F., Jablonski, K., Letcher, B., Hall, M., Tomkins-Tinch, C., Sochat, V., Forster, J., Lee, S., Twardziok, S., Kanitz, A., Wilm, A., Holtgrewe, M., Rahmann, S., Nahnsen, S., & Köster, J. (2021). Sustainable data analysis with Snakemake [version 2; peer review: 2 approved]. *F1000Research*, 10(33). <https://doi.org/10.12688/f1000research.29032.2>
- Nakayama, I., Foresti, F., Tewari, R., Schartl, M., & Chourrout, D. (1994). Sex chromosome polymorphism and heterogametic males revealed by two cloned DNA probes in the ZW/ZZ fish *Leporinus elongatus*. *Chromosoma*, 103(1), 31–39. <https://doi.org/10.1007/BF00364723>
- Popovic, I., & Riginos, C. (2020). Comparative genomics reveals divergent thermal selection in warm- and cold-tolerant marine mussels. *Molecular Ecology*, 29(3), 519–535. <https://doi.org/10.1111/mec.15339>
- Queirós, P., Delogu, F., Hickl, O., May, P., & Wilmes, P. (2021). Mantis: Flexible and consensus-driven genome annotation. *GigaScience*, 10(6), giab042. <https://doi.org/10.1093/gigascience/giab042>
- Quesada, H., Wenne, R., & Skibinski, D. O. F. (1995). Differential introgression of mitochondrial DNA across species boundaries within the marine mussel genus *Mytilus*. *Proceedings of the Royal Society B: Biological Sciences*, 262(1363), 51–56. <https://doi.org/10.1098/rspb.1995.0175>
- Quesada, H., Zapata, C., & Alvarez, G. (1995). A multilocus allozyme discontinuity in the mussel *Mytilus galloprovincialis*: The interaction of ecological and life-history factors. *Marine Ecology Progress Series*, 116, 99–115.
- Ranallo-Benavidez, T. R., Jaron, K. S., & Schatz, M. C. (2020). GenomeScope 2.0 and Smudgeplot for reference-free profiling of polyploid genomes. *Nature Communications*, 11(1), 1432. <https://doi.org/10.1038/s41467-020-14998-3>

- Shen, W., Le, S., Li, Y., & Hu, F. (2016). SeqKit: A Cross-Platform and Ultrafast Toolkit for FASTA/Q File Manipulation (Q. Zou, Ed.). *PLOS ONE*, 11(10), e0163962. <https://doi.org/10.1371/journal.pone.0163962>
- Simon, A., Arbiol, C., Nielsen, E. E., Couteau, J., Sussarellu, R., Burgeot, T., Bernard, I., Coolen, J. W. P., Lamy, J.-B., Robert, S., Skazina, M., Strelkov, P., Queiroga, H., Cancio, I., Welch, J. J., Viard, F., & Bierne, N. (2020). Replicated anthropogenic hybridisations reveal parallel patterns of admixture in marine mussels. *Evolutionary Applications*, 13(3), 575–599. <https://doi.org/10.1111/eva.12879>
- Simon, A., Fraïsse, C., El Ayari, T., Liautard-Haag, C., Strelkov, P., Welch, J. J., & Bierne, N. (2021). How do species barriers decay? Concordance and local introgression in mosaic hybrid zones of mussels. *Journal of Evolutionary Biology*, 34, 208–223. <https://doi.org/10.1111/jeb.13709>
- Skibinski, D. O. F., Ahmad, M., & Beardmore, J. A. (1978). Genetic evidence of naturally occurring hybrids between *Mytilus edulis* and *M. galloprovincialis*. 32(2), 354–364. <https://doi.org/10.1038/nature01240>
- Smit, A., Hubley, R., & Green, P. (2013–2015). *RepeatMasker Open-4.0* (Version 4.1.2-p1).
- Song, L., & Florea, L. (2015). Rcorrector: Efficient and accurate error correction for Illumina RNA-seq reads. *GigaScience*, 4(1), 48. <https://doi.org/10.1186/s13742-015-0089-y>
- Stanke, M., Diekhans, M., Baertsch, R., & Haussler, D. (2008). Using native and syntenically mapped cDNA alignments to improve de novo gene finding. *Bioinformatics*, 24(5), 637–644. <https://doi.org/10.1093/bioinformatics/btn013>
- Trizna, M. (2020). *Assembly_stats 0.1.4* (Version 0.1.4). <https://doi.org/10.5281/zenodo.3968775>
- Vasimuddin Md, S. M., Misra, S., Li, H., & Aluru, S. (2019). *Efficient Architecture-Aware Acceleration of BWA-MEM for Multicore Systems*.
- Walker, B. J., Abeel, T., Shea, T., Priest, M., Abouelliel, A., Sakthikumar, S., Cuomo, C. A., Zeng, Q., Wortman, J., Young, S. K., & Earl, A. M. (2014). Pilon: An Integrated Tool for Comprehensive Microbial Variant Detection and Genome Assembly Improvement. *PLOS ONE*, 9(11), 14.
- Weisenfeld, N. I., Kumar, V., Shah, P., Church, D. M., & Jaffe, D. B. (2017). Direct determination of diploid genome sequences. *Genome Research*, 27(5), 757–767. <https://doi.org/10.1101/gr.214874.116>
- Yang, J.-L., Feng, D.-D., Liu, J., Xu, J.-K., Chen, K., Li, Y.-F., Zhu, Y.-T., Liang, X., & Lu, Y. (2021). Chromosome-level genome assembly of the hard-shelled mussel *Mytilus coruscus*, a widely distributed species from the temperate areas of East Asia. *GigaScience*, 10. <https://doi.org/10.1093/gigascience/giab024>
- Zhang, S. V., Zhuo, L., & Hahn, M. W. (2016). AGOUTI: Improving genome assembly and annotation using transcriptome data. *GigaScience*, 5(1), 31. <https://doi.org/10.1186/s13742-016-0136-3>

393 **Supplementary Information**

394 **Tables**

Table S1: Steps carried out for each version of assembly

Version	Step	
v1	Raw assembly from Supernova	
v2	Supernova assembly using a filtered dataset of reads (section 2.3)	Unused
v3	Assembly with purged duplicates (purge_dups) from v3	
v4	Assembly with purged duplicates (purge_dups) from v1	
v5	Agouti repaired scaffolds from v4	
v6	Assembly with filtered contamination using Blobtoolkit results	
v7	Scaffolded assembly on <i>M. coruscus</i>	

395 **Figures**

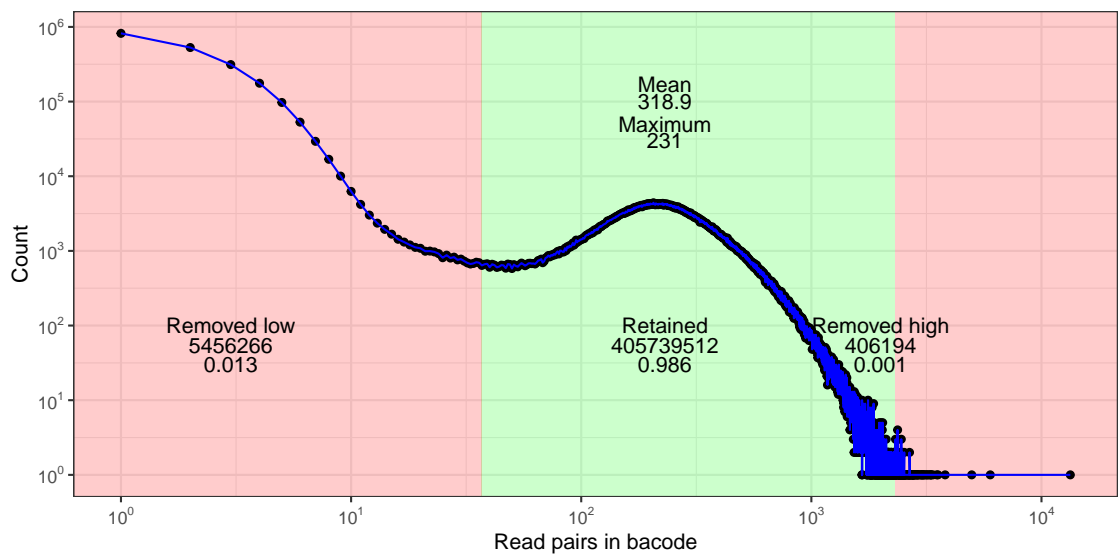


Figure S1: Histogram of read pairs identified for each 10X barcode for MgalMED. As part of preprocessing step, barcodes for which too few or too many read pairs are associated with each unique barcode are removed from the dataset (red regions).

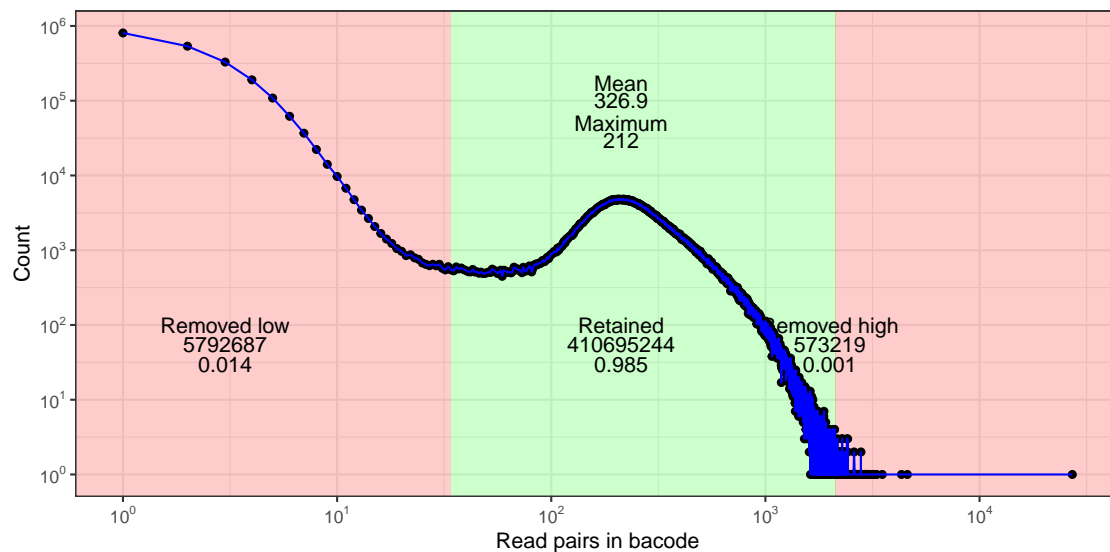


Figure S2: Histogram of read pairs identified for each 10X barcode for MeduEUS. As part of preprocessing step, barcodes for which too few or too many read pairs are associated with each unique barcode are removed from the dataset (red regions).

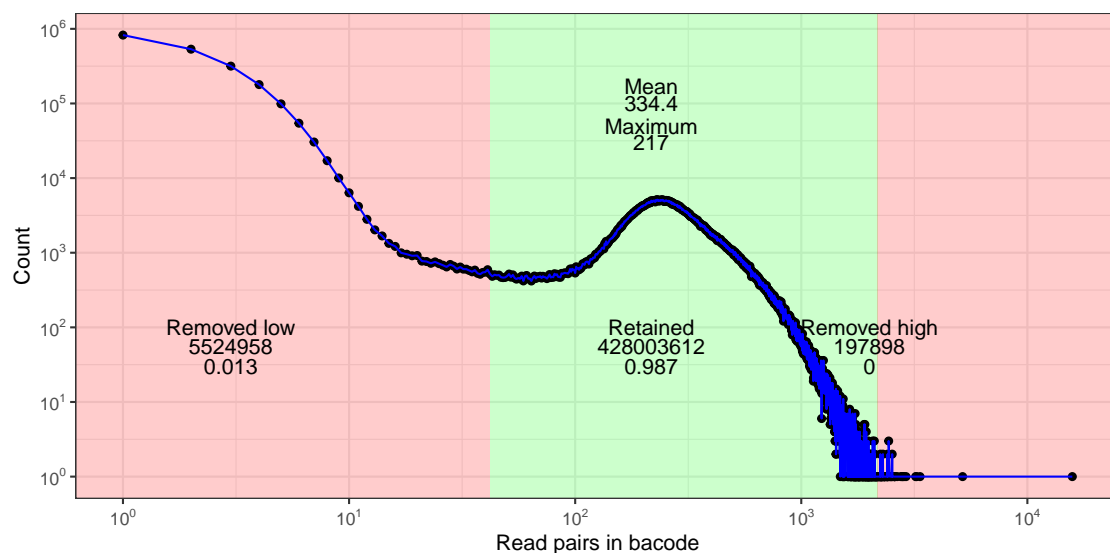


Figure S3: Histogram of read pairs identified for each 10X barcode for MeduEUN. As part of preprocessing step, barcodes for which too few or too many read pairs are associated with each unique barcode are removed from the dataset (red regions).

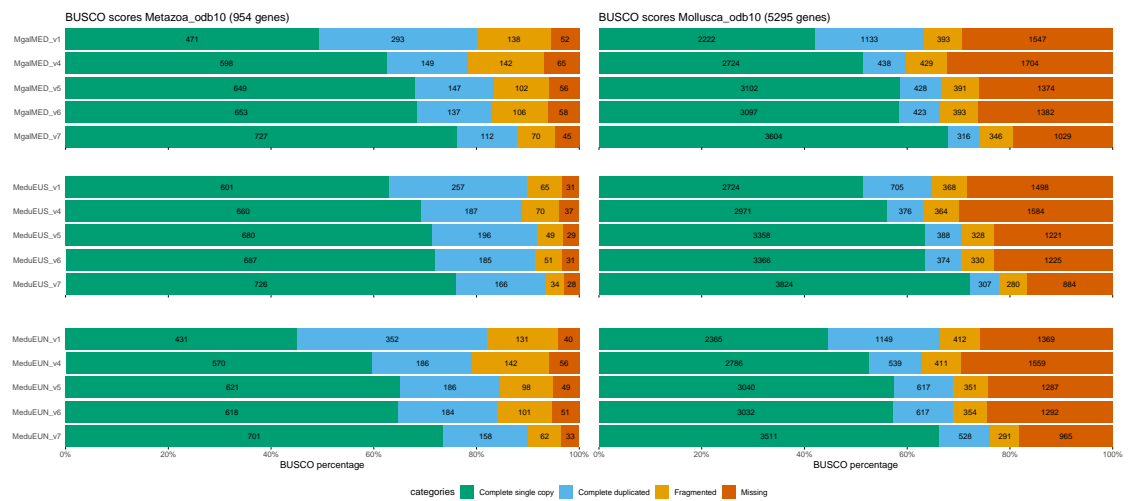


Figure S4: Busco scores on the metazoa_odb10 (left panels) and mollusca_odb10 (right panels) databases for each assembly MgalMED, MeduEUS and MeduEUN (top to bottom panels) across several assembly versions (v1, v4, v5, v6, v7).

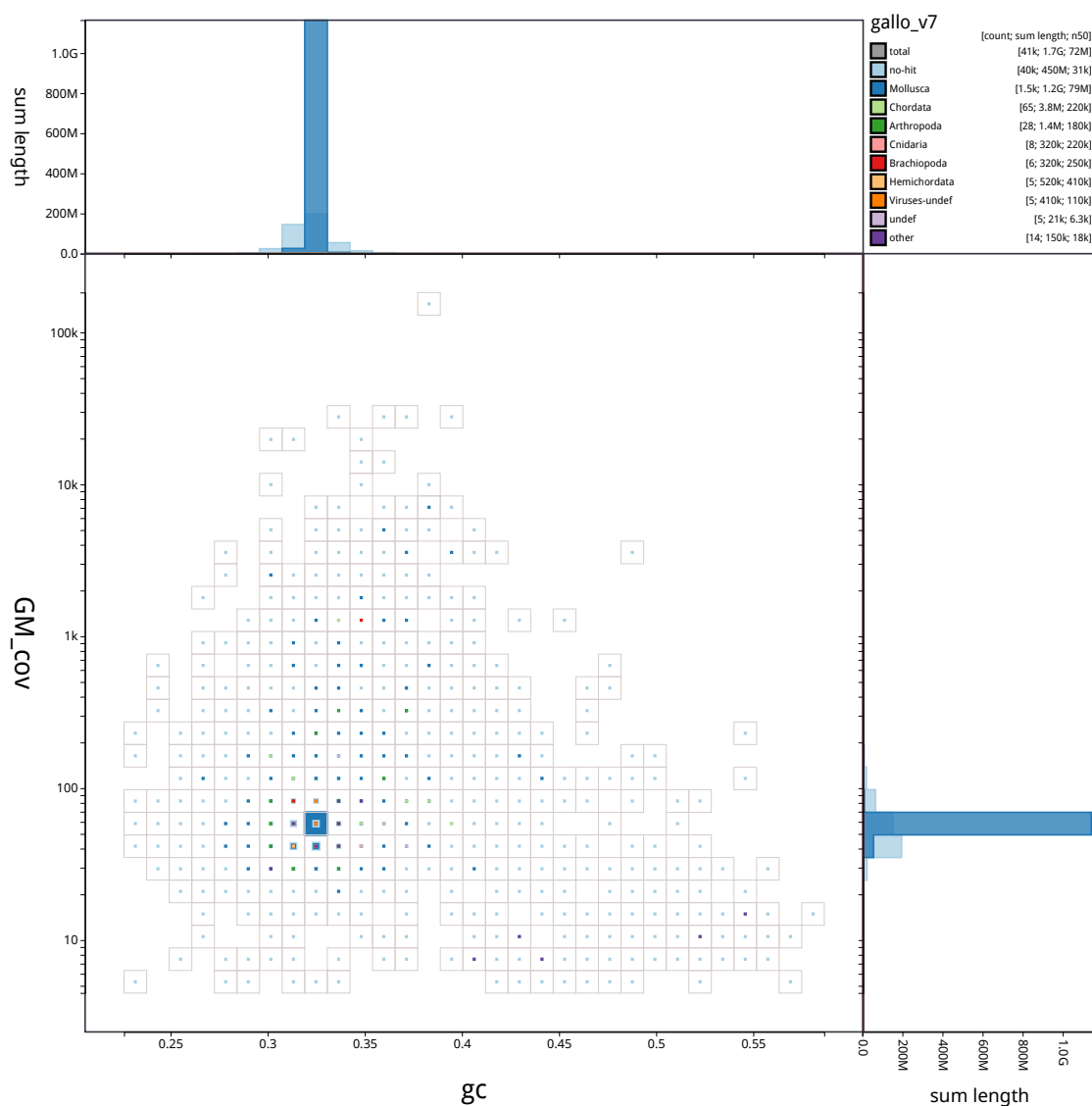


Figure S5: Blobtoolkit blob plot of base coverage in GM against GC proportion for scaffolds in assembly MgalMED_v7. Scaffolds are colored by phylum and binned at a resolution of 30 divisions on each axis. Colored squares within each bin are sized in proportion to the sum of individual scaffold lengths on a square-root scale, ranging from 1,005 to 1,127,105,406. Histograms show the distribution of scaffold length sum along each axis.

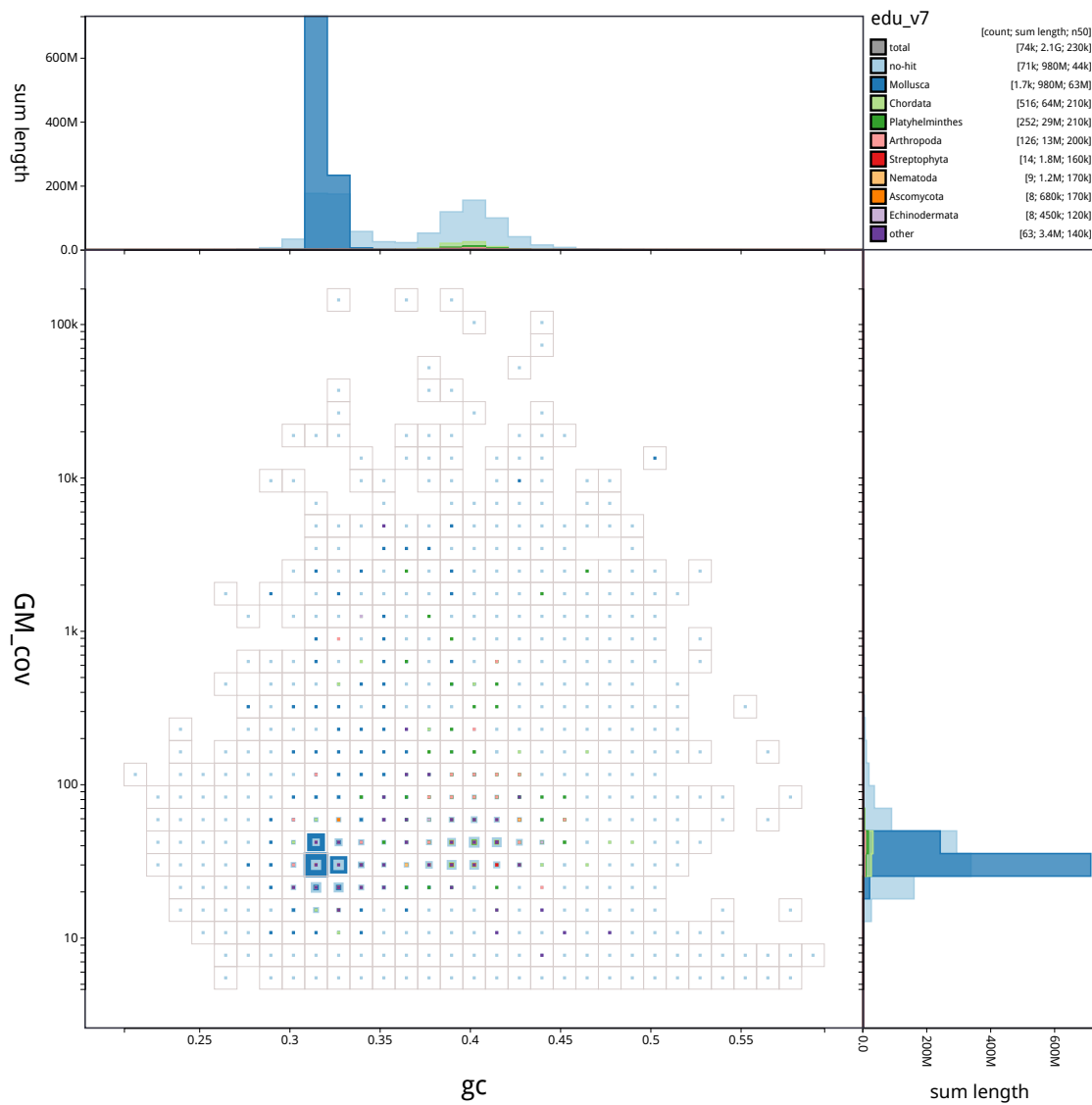


Figure S6: Blobtoolkit blob plot of base coverage in GM against GC proportion for scaffolds in assembly MeduEUS_v7. Scaffolds are colored by phylum and binned at a resolution of 30 divisions on each axis. Colored squares within each bin are sized in proportion to the sum of individual scaffold lengths on a square-root scale, ranging from 987 to 487,517,891. Histograms show the distribution of scaffold length sum along each axis.

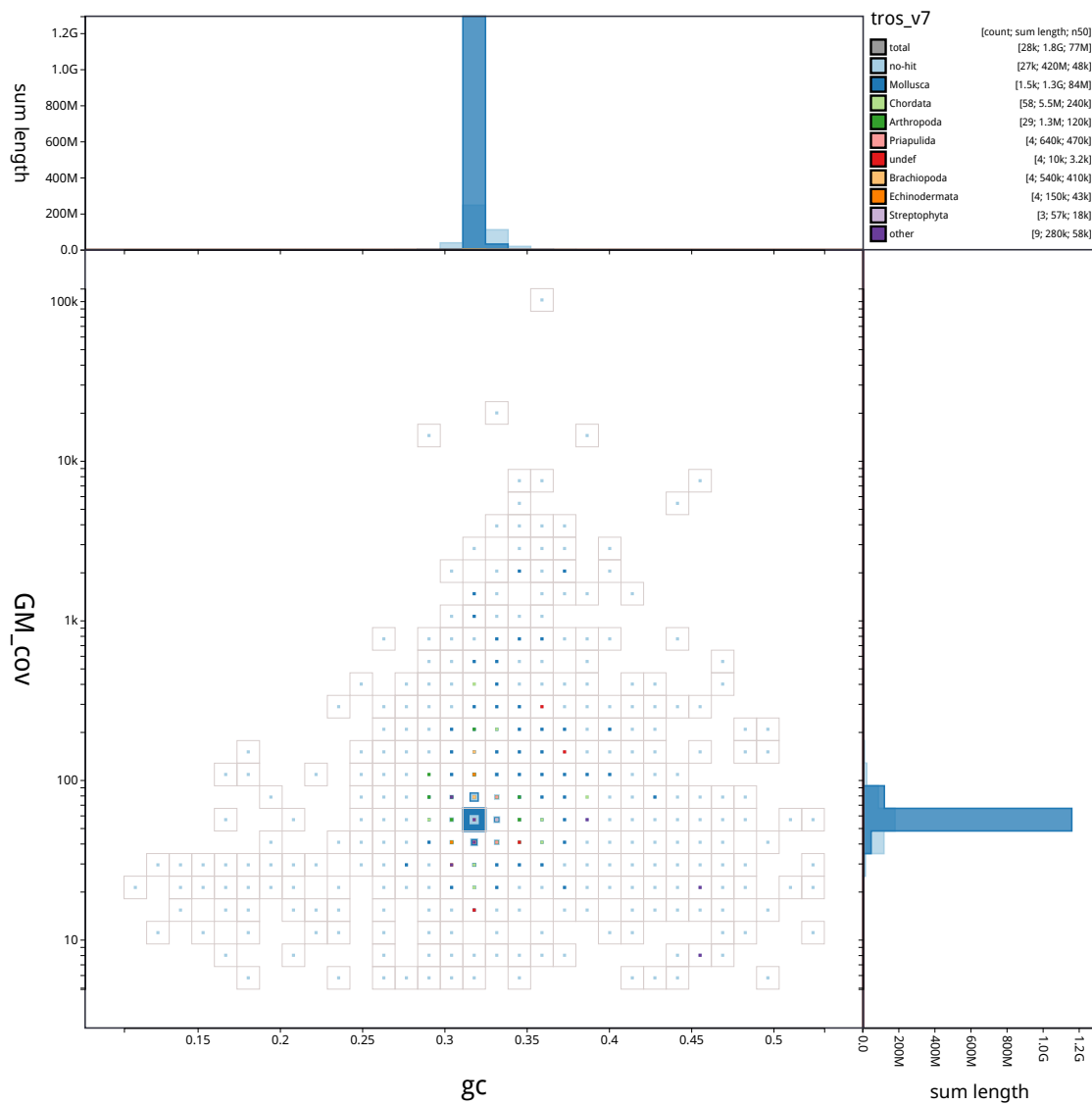


Figure S7: Blobtoolkit blob plot of base coverage in GM against GC proportion for scaffolds in assembly MeduEUN_v7. Scaffolds are colored by phylum and binned at a resolution of 30 divisions on each axis. Colored squares within each bin are sized in proportion to the sum of individual scaffold lengths on a square-root scale, ranging from 1,011 to 1,136,301,196. Histograms show the distribution of scaffold length sum along each axis.

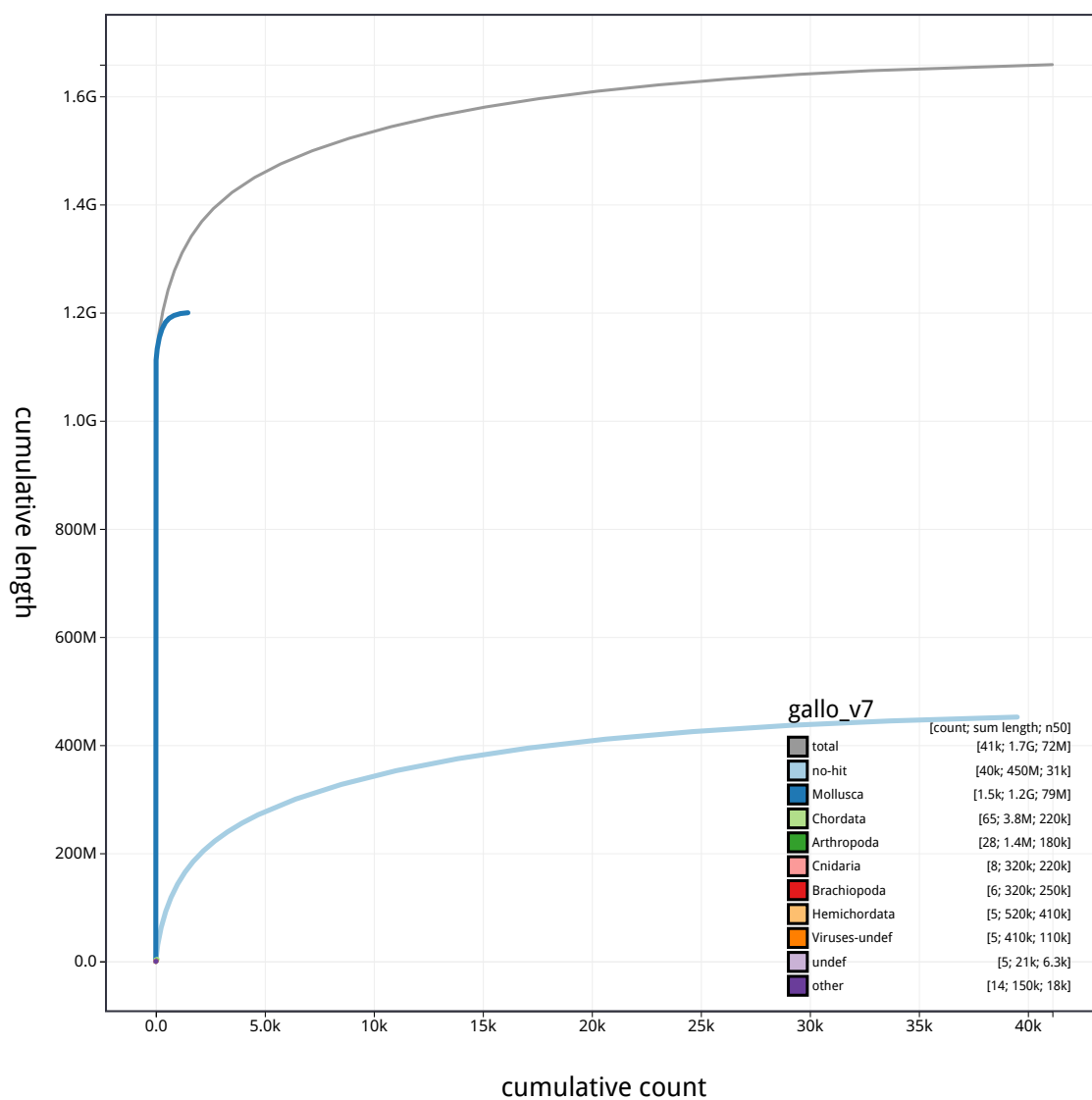


Figure S8: Blobtoolkit cumulative scaffold length for assembly MgalMED_v7. The gray line shows cumulative length for all scaffolds. Colored lines show cumulative lengths of scaffolds assigned to each phylum using the bestsumorder taxrule.

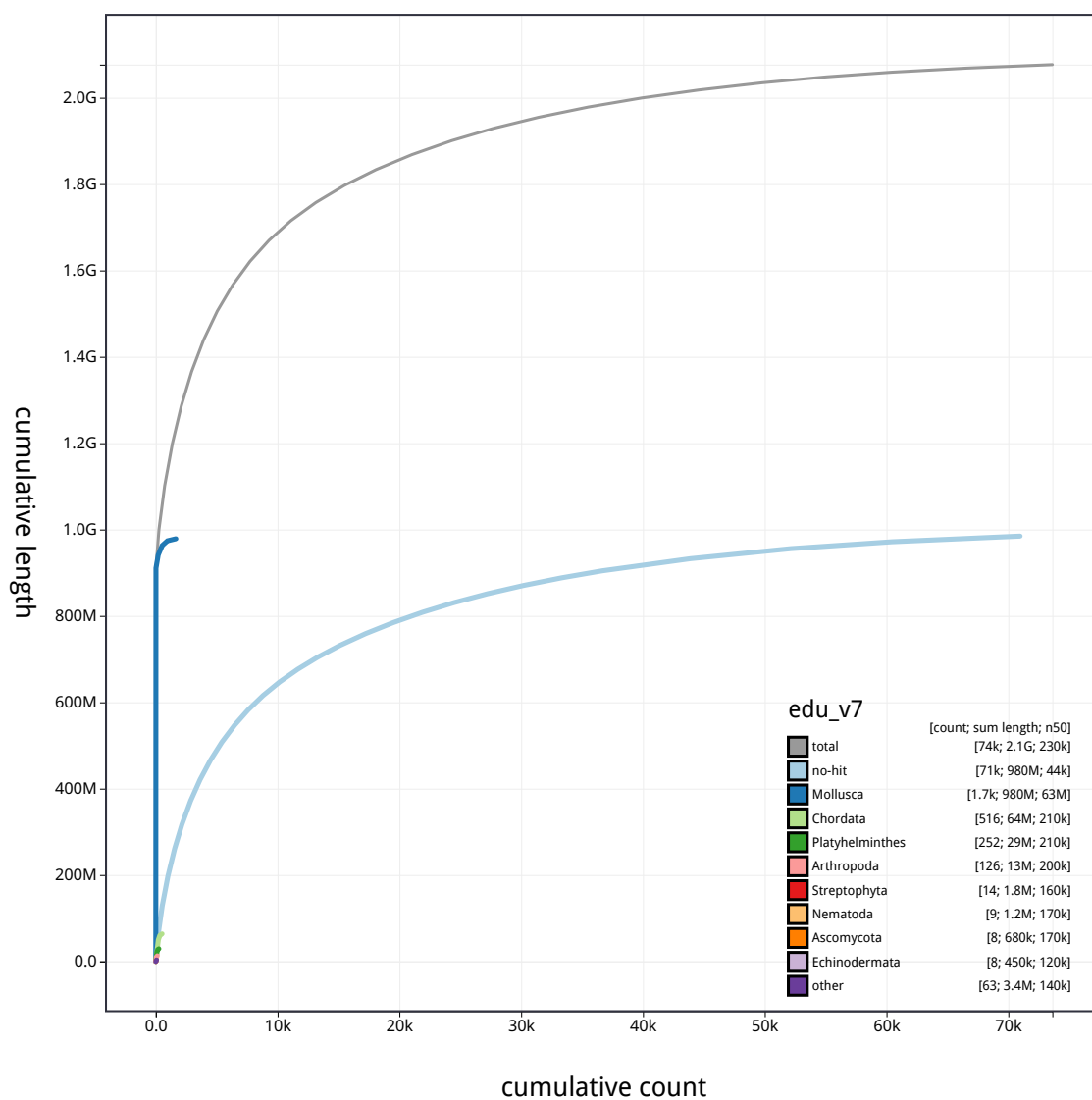


Figure S9: Blobtoolkit cumulative scaffold length for assembly MeduEUS_v7. The gray line shows cumulative length for all scaffolds. Colored lines show cumulative lengths of scaffolds assigned to each phylum using the bestsumorder taxrule.

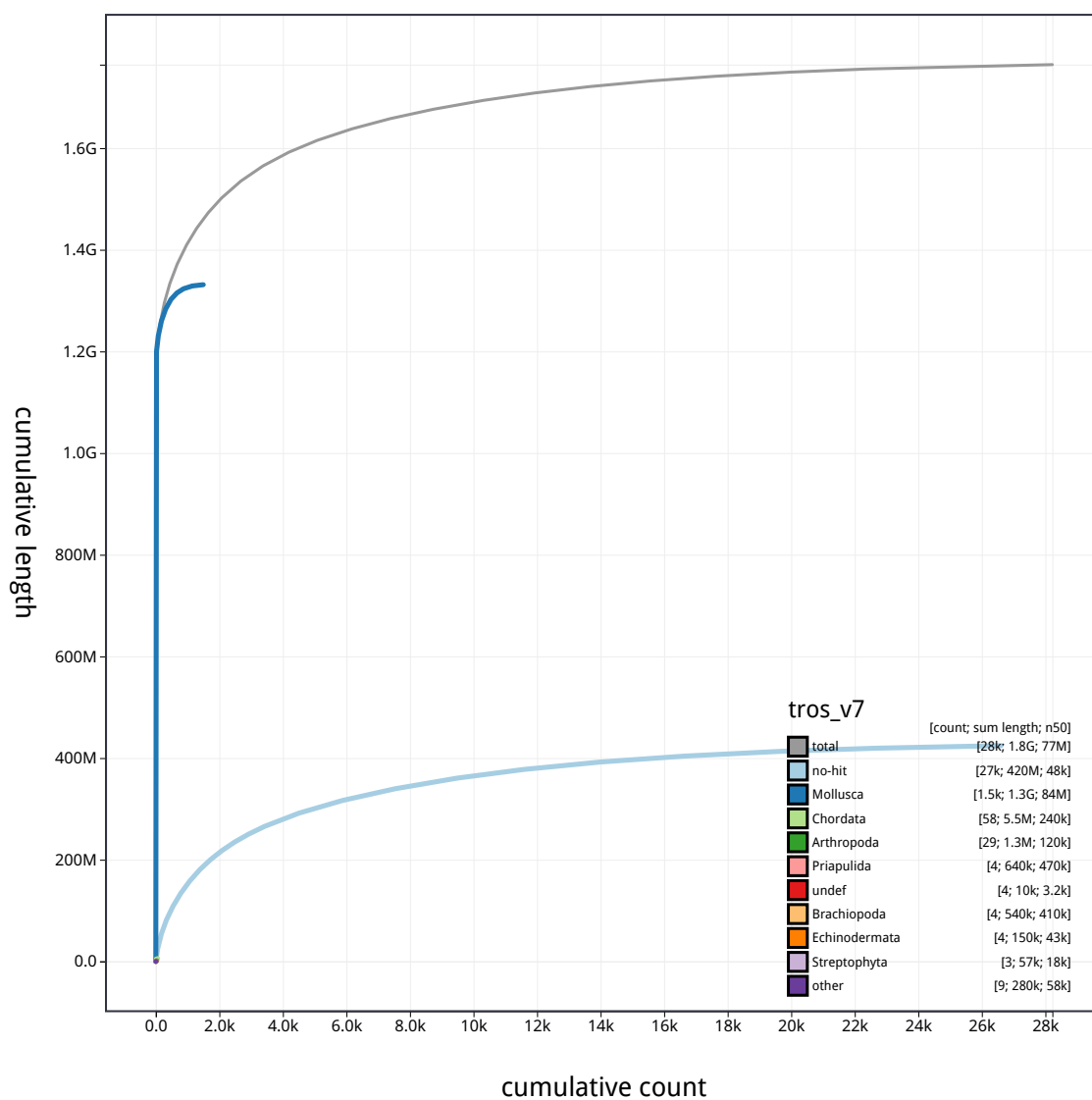


Figure S10: Blobtoolkit cumulative scaffold length for assembly MeduEUN_v7. The gray line shows cumulative length for all scaffolds. Colored lines show cumulative lengths of scaffolds assigned to each phylum using the bestsumorder taxrule.

Scaffold statistics

- Log10 scaffold count (total 41k)
- Scaffold length (total 1.7G)
- Longest scaffold (100M)
- N50 length (72M)
- N90 length (16k)

BUSCO

mollusca_odb10 (5295)

- Complete (74.0%)
- Fragmented (6.5%)
- Duplicated (6.0%)
- Missing (19.4%)

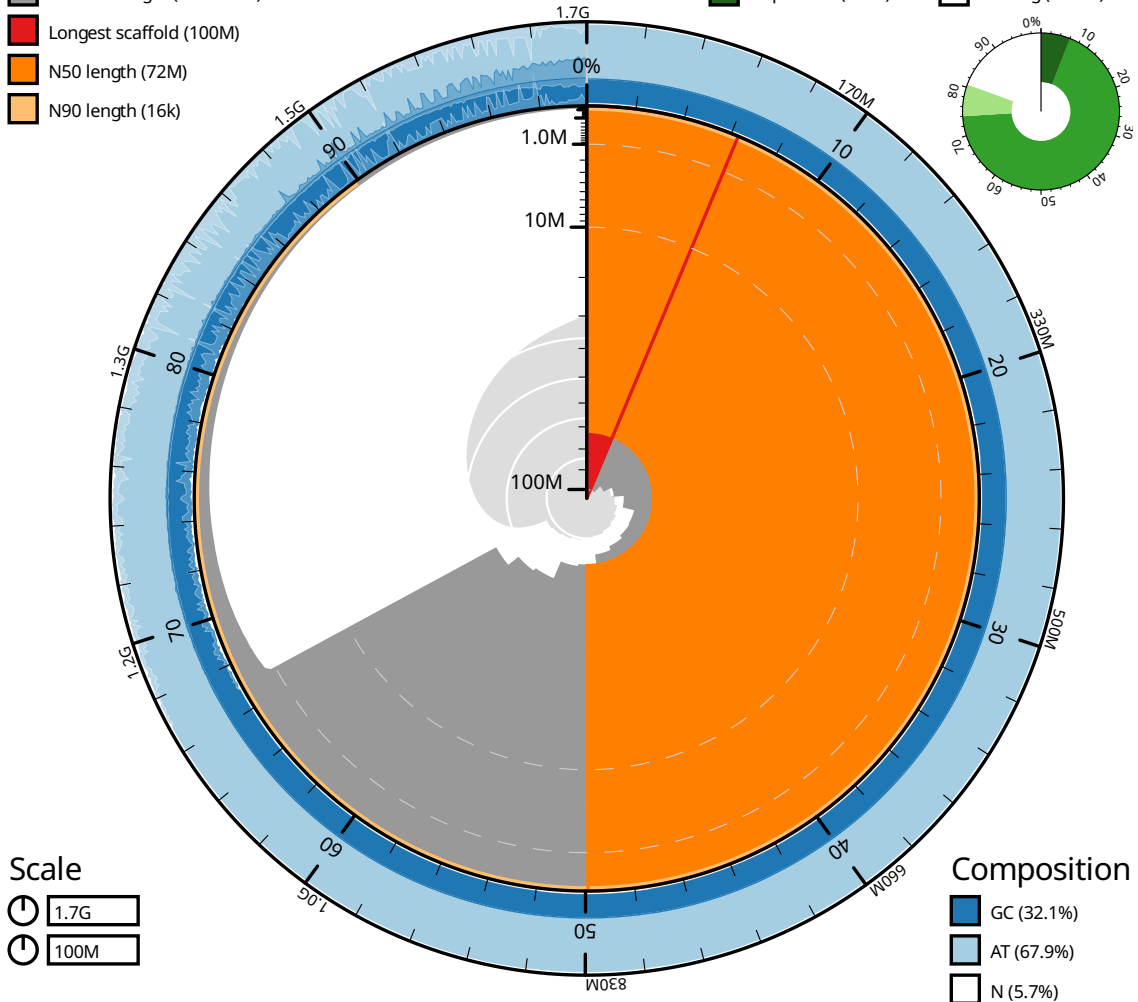


Figure S11: Blobtoolkit snail plot summary of assembly statistics for assembly MgalMED_v7. The main plot is divided into 1,000 size-ordered bins around the circumference with each bin representing 0.1% of the 1,658,656,017 bp assembly. The distribution of scaffold lengths is shown in dark gray with the plot radius scaled to the longest scaffold present in the assembly (104,729,878 bp, shown in red). Orange and pale-orange arcs show the N50 and N90 scaffold lengths (71,952,646 and 16,011 bp), respectively. The pale gray spiral shows the cumulative scaffold count on a log scale with white scale lines showing successive orders of magnitude. The blue and pale-blue area around the outside of the plot shows the distribution of GC, AT and N percentages in the same bins as the inner plot. A summary of complete, fragmented, duplicated and missing BUSCO genes in the mollusca_odb10 set is shown in the top right.

Scaffold statistics

- Log10 scaffold count (total 74k)
- Scaffold length (total 2.1G)
- Longest scaffold (88M)
- N50 length (230k)
- N90 length (11k)

BUSCO

mollusca_odb10 (5295)

- Complete (78.0%)
- Fragmented (5.3%)
- Duplicated (5.8%)
- Missing (16.7%)

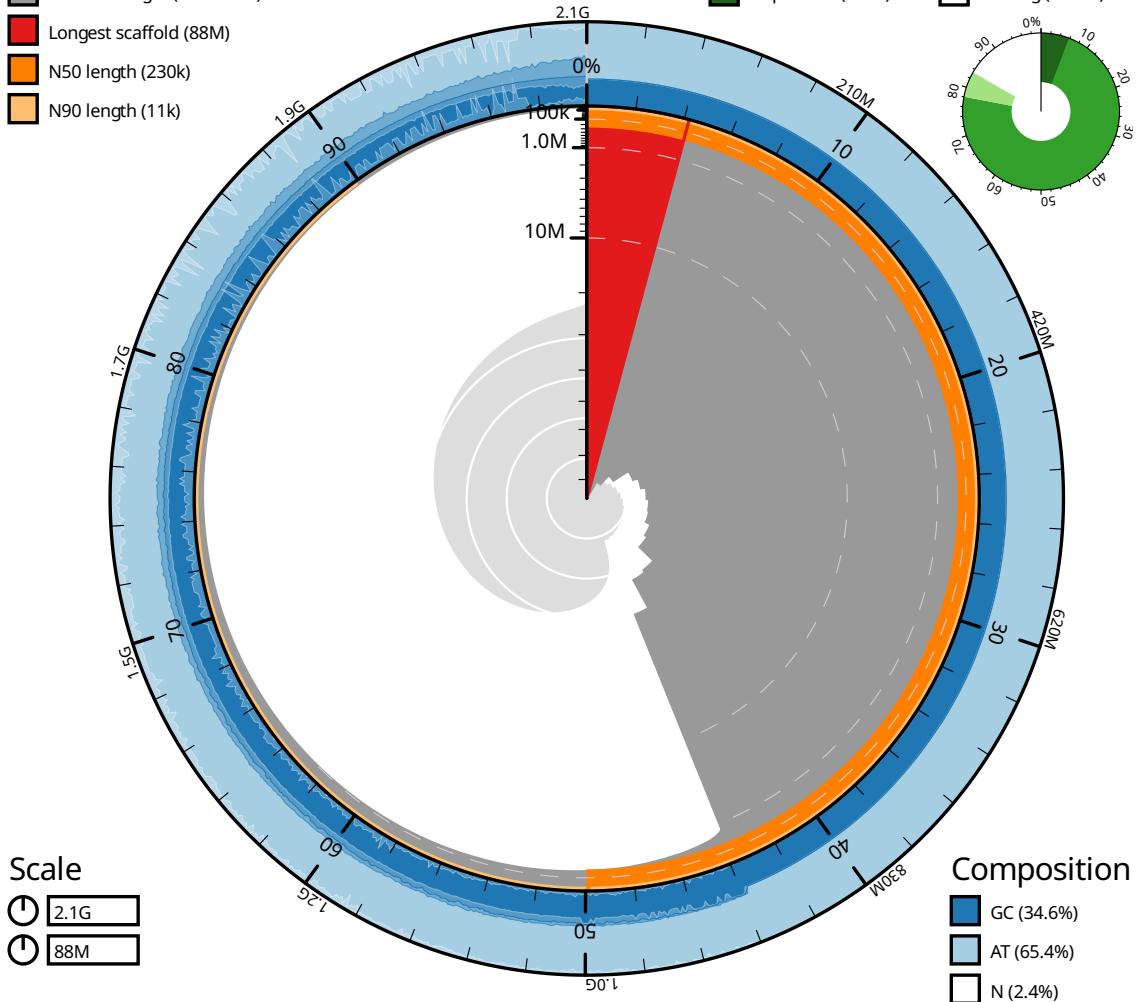


Figure S12: Blobtoolkit snail plot summary of assembly statistics for assembly MeduEUS_v7. The main plot is divided into 1,000 size-ordered bins around the circumference with each bin representing 0.1% of the 2,076,685,641 bp assembly. The distribution of scaffold lengths is shown in dark gray with the plot radius scaled to the longest scaffold present in the assembly (88,305,666 bp, shown in red). Orange and pale-orange arcs show the N50 and N90 scaffold lengths (228,263 and 10,773 bp), respectively. The pale gray spiral shows the cumulative scaffold count on a log scale with white scale lines showing successive orders of magnitude. The blue and pale-blue area around the outside of the plot shows the distribution of GC, AT and N percentages in the same bins as the inner plot. A summary of complete, fragmented, duplicated and missing BUSCO genes in the mollusca_odb10 set is shown in the top right.

Scaffold statistics

- Log10 scaffold count (total 28k)
- Scaffold length (total 1.8G)
- Longest scaffold (110M)
- N50 length (77M)
- N90 length (31k)

BUSCO

mollusca_odb10 (5295)

- Complete (76.3%)
- Fragmented (5.5%)
- Duplicated (10.0%)
- Missing (18.2%)

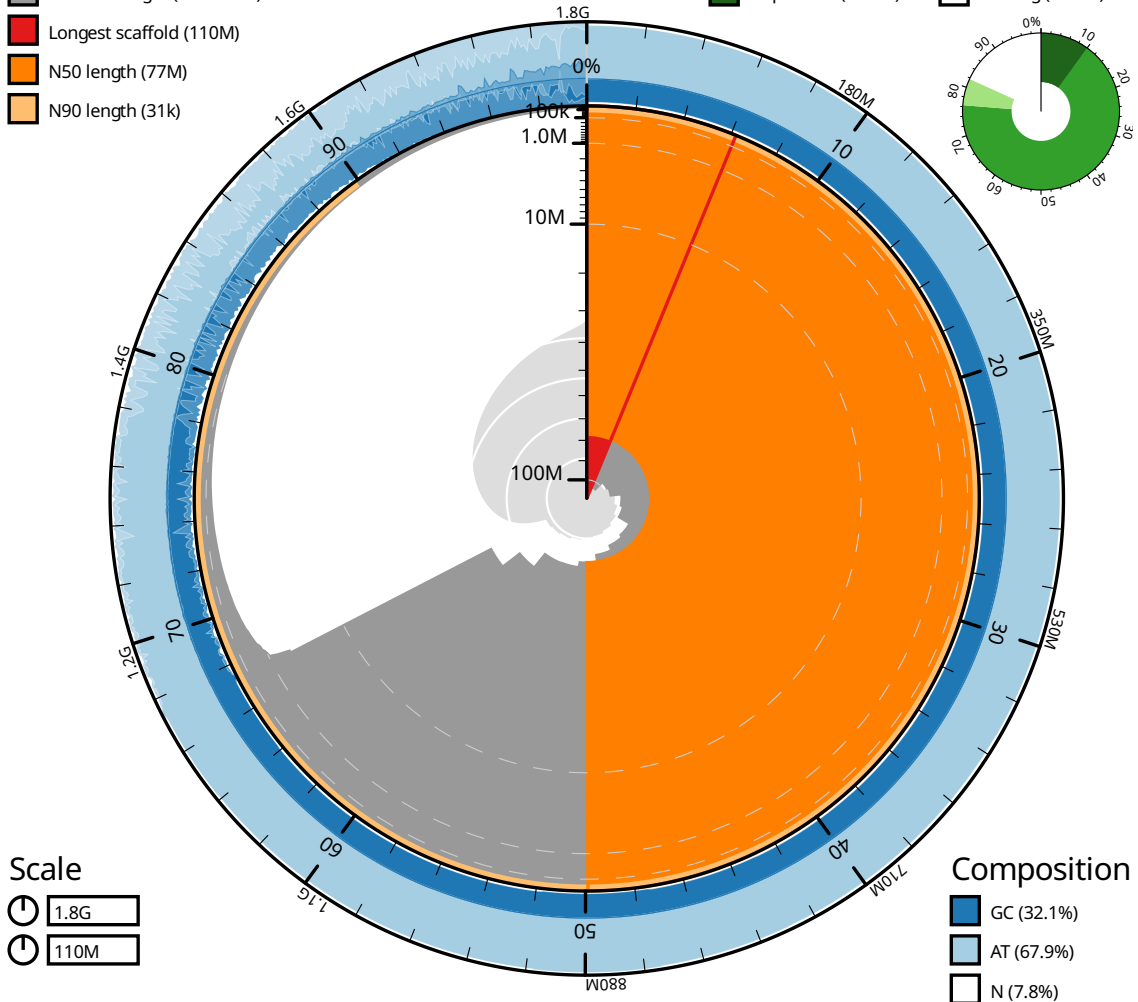


Figure S13: Blobtoolkit snail plot summary of assembly statistics for assembly MeduEUN_v7. The main plot is divided into 1,000 size-ordered bins around the circumference with each bin representing 0.1% of the 1,764,246,486 bp assembly. The distribution of scaffold lengths is shown in dark gray with the plot radius scaled to the longest scaffold present in the assembly (110,194,685 bp, shown in red). Orange and pale-orange arcs show the N50 and N90 scaffold lengths (77,102,752 and 30,649 bp), respectively. The pale gray spiral shows the cumulative scaffold count on a log scale with white scale lines showing successive orders of magnitude. The blue and pale-blue area around the outside of the plot shows the distribution of GC, AT and N percentages in the same bins as the inner plot. A summary of complete, fragmented, duplicated and missing BUSCO genes in the mollusca_odb10 set is shown in the top right.